The Hy Redshift Universe
ASP Conference Series, Vol. 193, 1999
A. J. Bunker & W. J. M. van Breugel, eds.

15 μm Extragalactic Surveys: Source Counts and Properties

D. Elbaz[1,2], C.J. Cesarsky[1,3], D. Fadda[1], H. Aussel[1,4], F.X. Désert[5], A. Franceschini[6], H. Flores[1], M. Harwit[7], J.L. Puget[8], J.L. Starck[1], L. Danese[9], D.C. Koo[10] and R. Mandolesi[11]

[1]*CEA-Saclay, SAp/DAPNIA/DSM,* [2]*UCSC, Physics Department, Santa Cruz, CA 95064, USA*

[3]*European Southern Observatory, Karl-Schwarzchild-Straße, 2 D-85748 Garching bei München, Germany*

[4]*Osservatorio di Padova, Vicolo Osservatorio, 5, I35122 Padova, Italy*

[5]*Observatoire de Grenoble, BP 53, 414 rue de la piscine, 38041 Grenoble Cedex 9, France*

[6]*Dipartimento di Astronomia, Università di Padova, Vicolo dell'Osservatorio, 5, I35122 Padova, Italy*

[7]*511 H Street S.W., Washington, DC 20024-2725; also Cornell University, USA*

[8]*Institut d'Astrophysique Spatiale, Université Paris XI, F-91405 Orsay Cédex, France*

[9]*SISSA, via Beirut 2-4, I-34013 Trieste , Italy*

[10]*UCO/Lick Obs., University of California, Santa Cruz, CA 95064, USA*

[11]*Bologna Radio Astronomy Institute, via Gobetti 101, 40129 Bologna, Italy.*

Abstract. We present the results of the five mid-infrared 15 μm (12-18 μm LW3 band) ISOCAM Guaranteed Time Extragalactic Surveys performed in the regions of the Lockman Hole and Marano Field. The roughly 1000 sources detected, 614 of which have a flux above the 80 % completeness limit, guarantee a very high statistical significance for the integral and differential source counts from 0.1 mJy up to ~5 mJy. By adding the ISOCAM surveys of the HDF-North and South (plus flanking fields) and the lensing cluster A2390 at low fluxes and IRAS at high fluxes, we cover four decades in flux from 50 μJy to ~0.3 Jy. The slope of the differential counts is very steep (α=-3.0) in the flux range 0.4-4 mJy, hence much above the Euclidean expectation (no expansion, no curvature) of α=-2.5. When compared with no-evolution models based on IRAS, our counts show a factor ~ 10 excess at 400 μJy, and a fast convergence, with α=-1.6, at lower fluxes.

They prolongate the IRAS image of the infrared universe four orders of magnitude fainter in the mid-IR. Being limited to redshifts below z$\sim$1.6 due to *k*-correction, the following results may not seem to reveal the nature of the 'high redshift universe' highlighted during this conference. However, we wish to demonstrate that they reveal a fundamental constituent in the understanding of galaxy evolution, namely the dust, which affects not only a few local ultra-luminous galaxies but probably most of the past star formation. The following text originates from Elbaz *et al.* (1999), except for the discussion of the nature of the 15 μm galaxies.

1. Introduction

Deep galaxy counts as a function of magnitude, or flux density, should, in principle, give a constraint on the geometry of the universe (Ω_o, Λ_o). In fact, their departure from the Euclidean expectation (no expansion, no curvature) is dominated by the *e*-correction (intrinsic evolution of the galaxies) and by the *k*-correction (redshift dependence). The understanding of galaxy evolution therefore is a key problem for cosmology. Number counts present the advantage of setting strong constraints on galaxy evolution models, without suffering from the peculiar behavior of each individual galaxy. In the local universe, galaxies radiate mainly in the optical-UV energy range (Soifer & Neugebauer 1991). If this remained true over the whole history of the universe, then one could follow the comoving star formation rate of the universe as a function of redshift by measuring the optical-UV light radiated by galaxies (Lilly *et al.* 1996, Madau *et al.* 1996).

This scenario changed considerably after the detection of a substantial diffuse cosmic infrared background (CIRB) in the 0.1 – 1 mm range from the COBE-FIRAS data (Puget *et al.* 1996, Guiderdoni *et al.* 1997, Hauser *et al.* 1998, Fixsen *et al.* 1998, Lagache *et al.* 1999) and at 140 – 240 μm from the COBE-DIRBE data (Hauser *et al.* 1998, Lagache *et al.* 1999). Surprisingly the mid-IR/sub-mm extragalactic background light is at least as large as that of the UV/optical/near-IR background (Dwek *et al.* 1998, Lagache *et al.* 1999), which implies a stronger contribution of obscured star formation at redshifts larger than those sampled by IRAS (limited to z<0.2). In order to understand the exact origin of this diffuse emission and its implications for galaxy evolution, it needs to be resolved into its individual galaxies which requires direct observations in the IR/sub-mm range (since correcting for dust extinction is a complex and non secure way).

Since dust emission starts to dominate the spectral energy distribution (SED) of most galaxies around 6 μm, the galaxies responsible for the CIRB must also appear in the mid-IR (i.e. 5-20 μm for ISOCAM) as long as their redshift is smaller than z$\sim$ 1.6. This is particularly true for luminous infrared galaxies (LIGs), which exhibit a bolometric luminosity greater than $10^{11}\,L_{\odot}$, mostly radiated in the infrared domain. While the detection of such galaxies was limited to the closeby universe with IRAS (z<0.2, Sanders & Mirabel 1996) because of its sensitivity, ISOCAM (Cesarsky *et al.* 1996), the camera on-board ISO (Kessler *et al.* 1996), with a thousand times better sensitivity and sixty times better spatial resolution, provides for the first time the opportunity to perform cosmologically meaningful surveys limited only by the disappearance of dust emission due to k-correction above z$\sim$1.6, instead of sensitivity. Deep surveys have been carried out on small fields containing sources well known at other wavelengths: the HDF North (Serjeant *et al.* 1997, Aussel *et al.* 1999, Désert *et al.* 1999) and the CFRS 1452+52 (Flores *et al.* 1999). This has yielded a small but meaningful sample of sources (83 galaxies) with a positional accuracy better than 6", sufficient for most multiwavelength studies. Optical counterparts are easily identifiable for these sources, precisely because their maximum redshift is limited by the k-correction to z$\sim$1.6, and that they appeared to be intrinsically bright ($L_{bol} \sim$ few 10^{11} $L_\odot$) and massive ($M \sim 10^{11}$ $M_\odot$, estimated from their optical and near-IR magnitudes) galaxies (Aussel *et al.* 1999a,b, Flores *et al.* 1999). Flores *et al.* (1999) estimate, from their sample of 41 sources, that accounting for the IR light from star forming galaxies may lead to a global star formation rate which is 2 to 3 times larger than assessed from UV light only.

To obtain reliable source count diagrams, better statistics and a wider range of flux densities are required. For this reason, we have performed several cosmological surveys with ISOCAM, ranging from large area-shallow surveys to small area-ultra deep surveys. These surveys were obtained in the two main broad-band filters LW2 (5-8.5 μm) and LW3 (12-18 μm), centered at 6.75 μm and 15 μm respectively. This paper only presents the source counts at 15 μm, because the sample of galaxies detected in the 6.75 μm band is strongly contaminated by Galactic stars, whose secure identification requires ground-based follow-up observations. Including the surveys over the two Hubble deep fields, almost 1000 sources with flux densities ranging from 0.1 mJy to 10 mJy were detected, allowing us to establish detailed source count diagrams.

We will not discuss the modeling of these source counts, since the strong evolution they revealed can hardly be reproduced by published models. However, we will discuss their compatibility with those obtained in the far-infrared with ISOPHOT, at 175 μm, and in the sub-millimeter with SCUBA, at 850 μm. In a second paper, published in these proceedings, we discuss these results in terms of extragalactic background light.

2. Description of the Surveys

The five ISOCAM Guaranteed Time Extragalactic Surveys (Cesarsky & Elbaz 1996) are complementary. They were carried out in both the northern (Lockman Hole) and southern (Marano Field) hemispheres, in order to be less biased by large-scale structures. These two fields were selected for their low zodiacal and cirrus emission and because they had been studied at other wavelengths, in particular in the X-ray band, which is an indicator of the AGN activity of the galaxies. Their features are summarized in the Table 1 below.

Only one of the 'Marano' maps was scanned at the exact position of the original Marano Field (Marano, Zamorani, Zitelli 1988), while the 'Marano FIRBACK' (MFB) Deep and Ultra-Deep were positioned at the site of lowest galactic cirrus emission, because they were combined with the FIRBACK ISOPHOT survey at 175 μm (Puget *et al.* 1999, Dole *et al.* 1999). Since the importance

Table 1. 15 μm ISOCAM deep surveys.

Survey Name (1)	N_{obs} (2)	Area (am^2) (3)	$S_{80\%}$ (mJy) (4)	t_{int} (min) (5)	# gal (6)	Slope (7)
Lockman Shallow[a]	3	1944	1	3	80	-2.1 ± 0.2
Lockman Deep[a]	6	510	0.6	11	70	-2.4 ± 0.3
MFB Deep[a]	18	710	0.4	15.4	144	-2.4 ± 0.2
Marano UD[a]	75	70	0.2	114	82	-1.5 ± 0.1
MFB UD[a]	75	90	0.2	114	100	-1.5 ± 0.2
HDF North[b]	64	27	0.1	135	44	-1.6 ± 0.2
HDF South[a]	64	28	0.1	168	63	-1.4 ± 0.1
A2390[c]	100	5.3	0.05	432	31	-1.2 ± 0.6

Comments: Col.(1) Survey name with reference: (a) in preparation, (b) Aussel *et al.* (1999), (c) Altieri *et al.* (1999); Col.(2) maximum number of pointings on the same sky position (redundancy); Col.(3) the total area covered in square arcminutes; Col.(4) the flux at which the survey is at least 80% complete; Col.(5) the corresponding integration time per sky position (in minutes); Col.(6) the number of galaxies whose flux is over the 80% completeness threshold; Col.(7) the slope of the fit to the integral $\log N - \log S$. A2390 completeness limit includes the corrections for lensing magnification.

of the Galactic cirrus emission in hampering source detection is much larger at 175$\,\mu$m than at 15$\,\mu$m, the quality of the two 15$\,\mu$m ultra deep surveys in the Marano Field area is equivalent. In addition, very deep surveys were taken with ISOCAM over the areas of the HDF North (Serjeant *et al.* 1997) and HDF South. In this paper, we include the HDF North results from Aussel *et al.* (1999), and show for the first time ISOCAM counts on the HDF South field.

3. Data Reduction and Simulations

The transient behavior of the cosmic ray induced glitches, which makes some of them mimic real sources, is the main limitation of ISOCAM surveys. We have developed two pipelines for the analysis of ISOCAM surveys in order to obtain two independent source lists per survey and improve the quality of the analysis. PRETI (Pattern REcognition Technique for ISOCAM data), developed by Starck *et al.* (1999), is able to find and remove glitches using multi-resolution wavelet transforms. It includes also Monte Carlo simulations to quantify the false detection rate, to calibrate the photometry and to estimate the completeness. The 'Triple Beam-Switch' (TBS) technique, developed by Désert *et al.* (1999), treats micro-scanning or mosaic images as if they resulted from beam-switching observations. All the surveys have been independently analyzed using both techniques and the source lists were cross-checked to attribute quality coefficients to the sources. PRETI and TBS agree at the 20 % level in photometry (corresponding to the photometric accuracy of both techniques), with an astrometric accuracy smaller than the pixel size (due to the redundancy). PRETI allowed us to attain fainter levels in deep surveys, whereas in the shallow surveys, where the redundancy is not very high, a very strict criterion of multiple

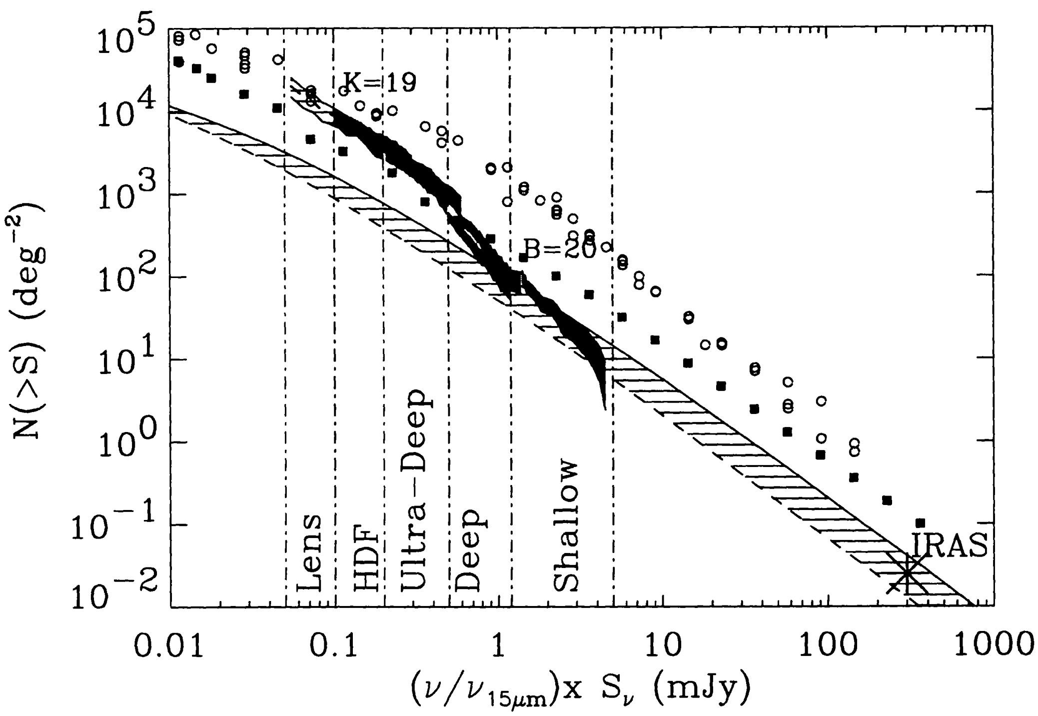

Figure 1. Integral counts, i.e. the number of galaxies, N, detected at 15 μm above the flux S(mJy), with 68 % confidence contours. K counts (Gardner et al. 1993) and B counts (Metcalfe et al. 1995),multiplied by the ratio ν/ν_{15} to represent the relative energy densities at high fluxes, are overplotted with open circles and filled squares , respectively. The hatched area materializes the range of possible expectations from models assuming no evolution and normalized to the IRAS 12 μm local luminosity function (LLF). The upper limit was calculated on the basis of the LLF of Rush, Malkan & Spinoglio (1993), as Xu *et al.* (1998) and shifted from 12 to 15 μm with the template SED of M82; the lower limit uses the LLF of Fang *et al.* (1998) and the template SED of M51.

detections had to be applied. Finally, we have made Monte Carlo simulations by taking into account completeness and photometric accuracy to correct for the Eddington bias and to compute error bars in the number count plots.

4. The ISOCAM 15 μm source counts

Figures 1 and 2 show respectively the integral and the differential number counts obtained in the five independent guaranteed time surveys conducted in the ISO-CAM 15 μm band, as well as the HDF surveys. The contribution of stars to the 15 μm counts was corrected. It is negligible at fluxes below the mJy level as confirmed by the spectro-photometric identifications in the ISOHDF-North (1 star out of 44 sources), South (3 stars over 71 sources), and CFRS 1415+52

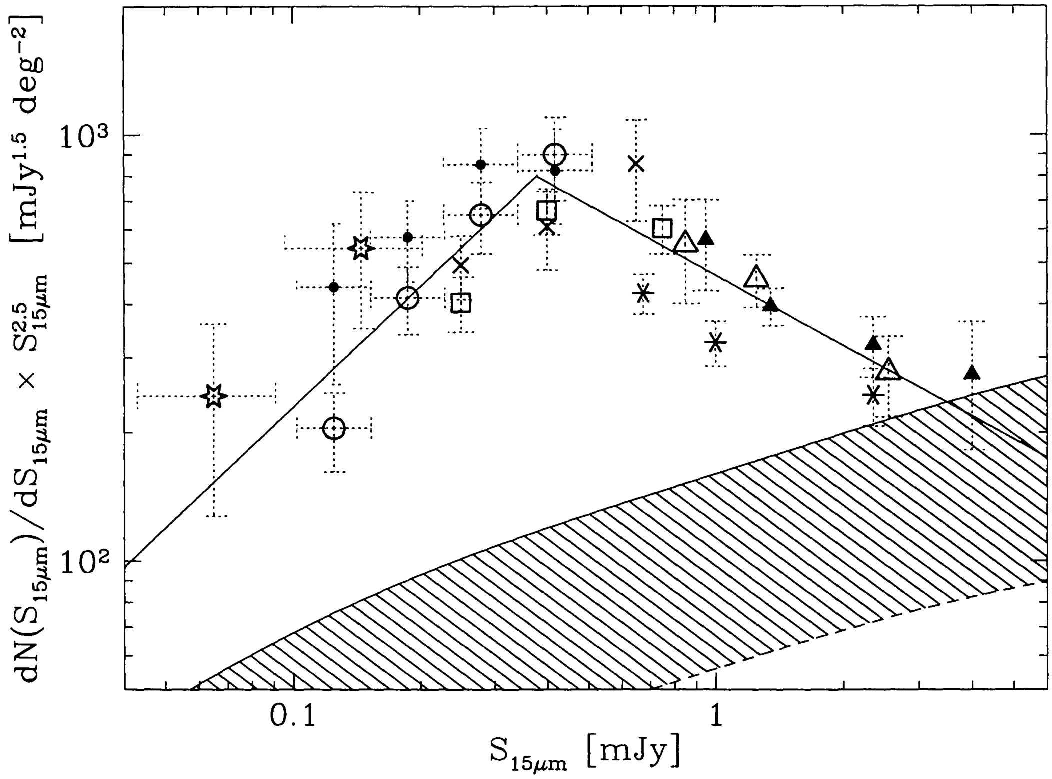

Figure 2. Differential Number Counts of 15 μm Galaxies, with 68% error bars. The counts are normalized to a Euclidean distribution of non-evolving sources, which would have a slope of α=-2.5 in such a universe. Data points: A2390 (open stars), ISOHDF-North (open circles), ISOHDF-South (filled circles), Marano FIRBACK (MFB) Ultra-Deep (open squares), Marano Ultra-Deep (crosses), MFB Deep (stars), Lockman Deep (open triangles), Lockman Shallow (filled triangles). The hatched area materializes the range of possible expectations from models assuming no evolution (see Fig.1).

(1 star over 41 sources ranging from ~0.3 mJy to ~0.8 mJy). In the Lockman Shallow Survey ($S_{15\mu m}$ > 1 mJy), about 12 % of the sources were classified as stars from their optical-mid IR colors (using the Rayleigh-Jeans law).

We have also represented the counts from the ISOHDF-North (from Aussel *et al.* 1999), ISOHDF-South, and, at the lowest fluxes, the counts obtained from the A2390 cluster lens (down to 50 μJy, corrected for the lensing effect; Altieri *et al.* 1999, see also Metcalfe *et al.* 1999). We have only included the flux bins where the surveys are at least 80 % complete, according to the simulations.

The first striking result of these complementary source counts is the consistency of the eight 15 μm surveys over the full flux range. Some scatter is nevertheless apparent; given the small size of the fields surveyed, we attribute some of it to clustering effects.

The two main features of the observed counts are a significantly super-euclidean slope (α=-3.0) from 3 to 0.4 mJy and a fast convergence at flux densities fainter than 0.4 mJy. In particular, the combination of five independent surveys in the flux range 90-400 μJy shows a turnover of the normalized differential counts around 400 μJy and a decrease by a factor ~3 at 100 μJy. We believe that this decrease, or the flattening of the integral counts below ~400 μJy, is real. It cannot be due to incompleteness, since this has been estimated from the Monte-Carlo simulations (see Section 3.). The differential counts can be fitted by two power laws by splitting the flux axis in two regions around 0.4 mJy. In units of mJy^{-1} deg^{-2}, we obtain, by taking into account the error bars:

$$\frac{dN(S)}{dS} = \begin{cases} (2000 \pm 600) \quad S^{(-1.6\pm0.2)} & \ldots \quad 0.1 \leq S \leq 0.4 \\ (470 \pm 30) \quad S^{(-3.0\pm0.1)} & \ldots \quad 0.4 \leq S \leq 4 \end{cases} \quad (1)$$

In the integral plot (Fig. 1), the curves are plotted with 68 % confidence contours based on our simulation analysis. The total number density of sources detected by ISOCAM at 15 μm is (4.2 ± 1.1) arcmin^{-2} down to 60 μJy (accounting for lensing) or (2.35 ± 0.3) arcmin^{-2} down to 100 μJy, using only direct flux density measurements.

5. Discussion of the number counts

We have presented the 15 μm differential and integral counts drawn by several complementary ISOCAM deep surveys, with a significant statistical sampling (993 galaxies, 614 of which have a flux above the 80 % completeness limit) over two decades in flux from 50 μJy up to 5 mJy. The differential counts (Fig. 2), which are normalized to S$^{-2.5}$, the expected differential counts in a non expanding Euclidean universe with sources that shine with constant luminosity, present a turnover around $S_{15\,\mu m}$=0.40 mJy, above which the slope is very steep (α=-3.0±0.1). No evolution predictions were derived assuming a pure *k*-correction in a flat universe (q_0=0.5), including the effect of Unidentified Infrared Band emission in the galaxy spectra. In the Figures, the lower curve is based on the Fang *et al.* (1998) IRAS 12 μm local luminosity function (LLF), using the spectral template of a quiescent spiral galaxy (M51). The upper curve is based on the Rush, Malkan and Spinoglio (1993) IRAS-12 μm LLF, translated to 15 μm using as template the M82 spectrum. We consider that, in the absence of a well established LLF at 15 μm, these two models can be considered as upper and lower bounds to the actual no-evolution expectations; note that the corresponding slope is ~-2. The actual number counts are well above these predictions; in the 0.3 mJy to 0.6 mJy range, the excess is around a factor 10: clearly, strong evolution is required to explain this result.

In Fig. 1, we have overplotted the integral counts in the K (from Gardner *et al.* 1993) and B (Metcalfe *et al.* 1995) bands, in terms of νS_ν. For bright sources, with densities lower than 10 deg$^-$2,these curves run parallel to an interpolation between the ISOCAM counts presented here and the IRAS counts; the bright K sources emit about ten times more energy in this band than a comparable number of bright ISOCAM sources at 15 μm. But the ISOCAM integral counts present a rapid change of slope around 1-2 mJy, and their numbers

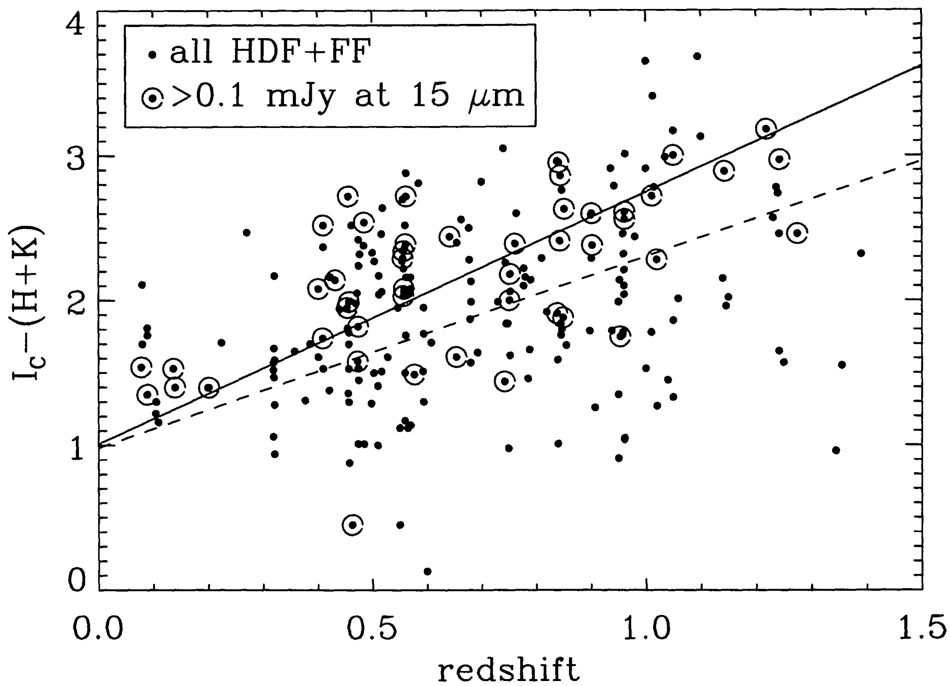

Figure 3. I(Kron-Cousins)-(H+K) color (from Cowie *et al.* 1999) versus redshift for field galaxies (dots) and galaxies detected above 0.1 mJy at 15 μm by ISOCAM (dots surrounded by circles), in the Hubble Deep Field North plus its Flanking Fields. Plain line: linear fit to the colors of ISOCAM galaxies. Dashed line: fit for all galaxies.

rise much faster than those of the K and B sources. The sources detected by ISOCAM are a sub-class of the K and B sources which harbor activity hidden by dust, and their proportion is higher among the faint sources.

6. Discussion of the nature of the 15 μm galaxies

We believe, according to the results obtained on the HDF and CFRS fields (Aussel *et al.* 1999; Flores *et al.* 1999), that the sources responsible for the 'bump' in the 15 μm counts are not the faint blue galaxies which dominate the optical counts and have a median redshift around z~0.6 (Pozzetti *et al.* 1998). Indeed, as shown in the Fig. 3, the galaxies from the HDF-N plus Flanking Fields whose 15 μm flux density is greater than 0.1 mJy (sensitivity limit of ISOCAM) harbour a I_C-(H+K) color distribution very similar to that of the whole sample of galaxies for which we have access to both the I_C-(H+K) colors and spectroscopic redshifts (from Cowie *et al.* 1999, where the index C is for Kron-Cousins). Aussel *et al.* (1999, PhD thesis and paper in preparation) showed that the sub-sample of galaxies with known spectroscopic redshift keeps

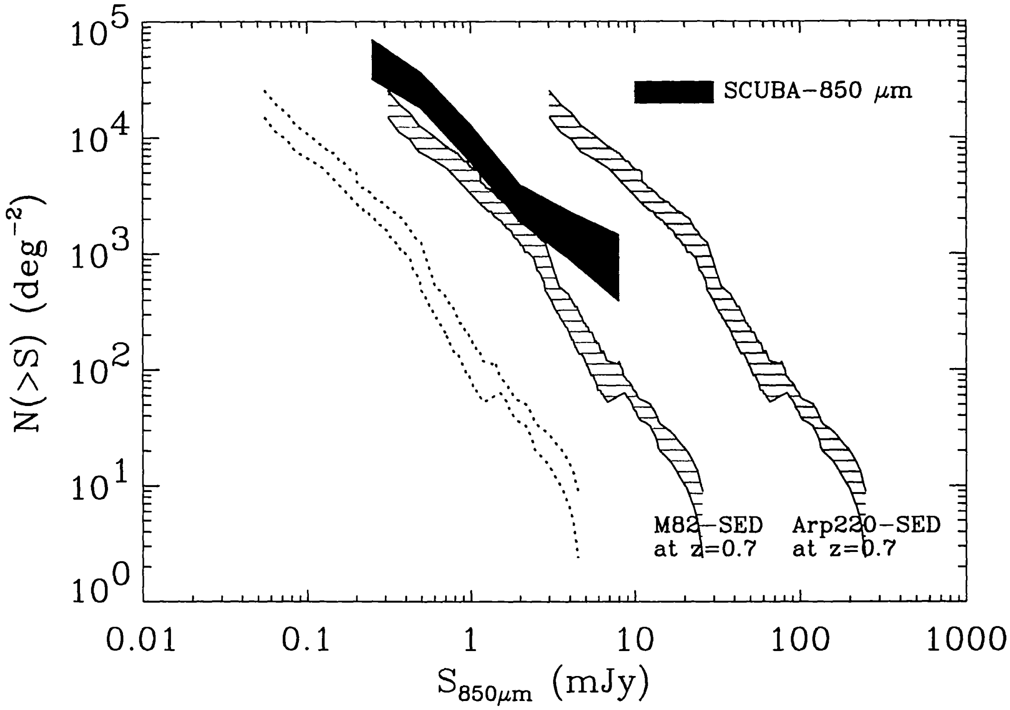

Figure 4. Integral counts at 850 μm from SCUBA (Blain *et al.*, these proceedings). From the 15 μm ISOCAM counts (dotted lines), one can extrapolate the contribution of the ISOCAM galaxies at 850 μm for a given redshift distribution and spectral energy distribution (SED). Two examples are shown here using the SEDs of M82 and Arp 220, and assuming that all ISOCAM galaxies have the same redshift, z=0.7, corresponding to their median redshift in the HDF and CFRS fields.

the same color properties than the full sample of HDF+FF galaxies, hence we did not include a selection bias in the color distribution.

The median colors are I_C-(H+K)= 2.3 for the 15 μm galaxies and I_C-(H+K)= 2 for all galaxies. However, the linear fit to the I_C-(H+K) versus redshift plot of the two samples of galaxies in Fig. 3 shows that the 'dusty' galaxies tend to redden slightly faster with increasing redshift, than the natural reddening of the whole population of field galaxies which is due to *k*-correction. Nevertheless, this difference is not strong enough to allow one to separate the infrared galaxies from the whole sample like for Lyman-break galaxies (even accounting for the other set of optical colors existing for the HDF galaxies). The origin of this reddening with redshift is not clear but it is probably due to a selection of the galaxies suffering from more extinction, hence emitting more in the infrared, at larger redshifts.

From the full sample of 15 μm galaxies with known redshift and optical-near IR magnitudes, we found that these galaxies are massive ($\sim 10^{11}\ M_\odot$) and that their emission occurs essentially in the IR and could account for a considerable part of the star formation in the universe at z<1.5 (Flores *et al.* 1999). Their median redshift is z∼0.8 in a sample of 42 galaxies brighter than 0.1 mJy in the HDF+FF (Aussel *et al.* 1999) and z∼0.7 in a sample of 41 galaxies brighter than 0.35 mJy in the CFRS-1415 field (Flores *et al.* 1999). The assessment of their bolometric luminosity requires the assumption of a spectral energy distribution, which is largely uncertain since the ratio of the far-IR over mid-IR flux densities is highly variable among galaxies. However, one can set limits to the bolometric luminosity using the following arguments. If all galaxies had extreme SEDs like the one of Arp220, they would produce a contribution to the SCUBA-850 μm number counts (see Blain *et al.*, these proceedings) much above observations (see Fig. 4). We show in a second paper presented in these proceedings about the 15 μm extragalactic background light (EBL) that Arp220-like SEDs can also be rejected for over-producing the 140 μm EBL with respect to the one measured by DIRBE on-board COBE. The light radiated in the far-IR by these galaxies however cannot be much lower than that emitted at 15 μm, since only galaxies luminous in the IR can be detected at z>0.5 with a 15 μm flux density larger than 0.1 mJy (the origin of the emission cannot be stellar without requiring excessive masses). We therefore estimated the mean bolometric luminosity of these galaxies to be of the order of a few 10^{11} $L_{\odot}$. Hence the population of galaxies producing the 15 μm number counts excess is very distinct from the one which dominates the deep optical counts, known to be made of low mass galaxies with blue luminosities, although at a similar redshift. In other words, the star formation activity responsible for the light emitted by the 15 μm galaxies is not the other face of the same star formation activity already quantified from the optical surveys, but instead should be considered as a second component, which was previously missed.

Linking luminosity to distance, we predict a rapid change of the luminosity function with increasing redshift, which can only be confirmed by a complete ground-based spectro-photometric follow-up. We should be able to follow the evolution of the luminosity function from z∼0.2 to 1.5 with the large number of galaxies detected in the Marano Field surveys. The combination of the intensity of the H_{α} emission line (redshifted in the J-band) with the IR luminosity could set strong constraints on the star formation rate. Finally, emission line diagnostics, combined with hard X-ray observations with XMM and Chandra, would allow us to understand whether the dominant source of energy is star formation or AGN activity.

References

Altieri B., Metcalfe L., Kneib J.P., 1999, A&A 343L, 65

Aussel H., Cesarsky C., Elbaz D., *et al.*, 1999a, A&A 342, 313

Aussel H., Cesarsky C., Elbaz D., *et al.*, 1999b, In "The Universe as seen by ISO", eds.: P.Cox, M.F.Kessler, ESA Publication Division, ESTEC, Noordwijk, NL

Cesarsky C., Abergel A., Agnèse P., *et al.*, 1996, A&A 315, L32

Cesarsky C.J., Elbaz D., 1996, IAUS, M. C. Kafatos, Y. Kondo (eds.), Kluwer Acad. Pub., Dordrecht, vol. 168, 109.

Cowie L.L., Clowe D., Fulton E., *et al.*, 1999, AJ, in preparation

Désert F.X., Puget J.L., Clements D., *et al.*, 1999, A&A 342, 363

Dole H., Lagache G., Puget J.L., *et al.*, 1999, in Cox, P., Kessler, M.F. (eds.), *The Universe as seen by ISO*, ESA SP-427, p. 1031, astro-ph/9902122

Dwek E., Arendt R.G., Hauser M.G., *et al.*, 1998, ApJ 508, 106

Elbaz D., Cesarsky C.J., Fadda, D., *et al.*, 1999, to appear in A&A Letter

Fang F., Shupe D., Xu C., Hacking P., 1998, ApJ 500, 693

Fixsen D.J., Dwek E., Mather J.C., *et al.*, 1998, ApJ 508, 123

Flores H., Hammer F., Thuan T., *et al.*, 1999, ApJ 517, 148

Franceschini A., *et al.*, 1999, in preparation

Gardner J.P., Cowie L.L., Wainscoat R.J., 1993, ApJ 415, L9

Guiderdoni B., Bouchet F, Puget J.L., *et al.*, 1997, Nat 390, 257

Hauser M.G., Arendt R.G., Kelsall T., 1998, ApJ 508, 25

Kessler M., Steinz J., Anderegg M., *et al.*, 1996, A&A 315, L27

Lagache G., Abergel A., Boulanger F., *et al.*, 1999, A&A 344, 322

Lilly S., Le Fèvre O., Hammer F., *et al.*, 1996, ApJ 460, L1

Madau P., Ferguson H., Dickinson M., *et al.*, 1996, MNRAS 283, 1388

Marano, B., Zamorani, G., Zitelli, V., 1988, MNRAS 232, 111

Metcalfe L., Altieri B., McBreen B., *et al.*, 1999, In "The Universe as seen by ISO", eds.: P.Cox, M.F.Kessler, ESA Publication Division, ESTEC, Noordwijk, NL

Metcalfe N., Shanks T., Fong R., *et al.*, 1995, MNRAS 273, 257

Pozzetti L., Madau P., Zamorani G., Ferguson H.C., Bruzual G.A., 1998, MNRAS, 298, 1133

Puget J.L. , Abergel A., Bernard J.P., *et al.*, 1996, A&A 308, L5

Puget J.L., Lagache G., Clements D., *et al.*, 1999, A&A 345, 29

Rush B., Malkan M.A., Spinoglio L., 1993, ApJS 89, 1

Sanders, D.B., Mirabel, I.F., 1996, *Ann. Rev. Astron. Astrophys.* 34, 749

Serjeant S., Eaton N., Oliver S., *et al.*, 1997, MNRAS 289, 457

Soifer B.T., Neugebauer G., 1991, AJ 101, 354

Starck J.-L., Aussel H., Elbaz D., *et al.*, 1999, A&AS 138, 365

Xu C., Hacking P., Fang F., *et al.*, 1998, ApJ 508, 576